EXPERIMENTAL AND THEORETICAL THREE-PHASE RELATIVE PERMEABILITY FOR WAG INJECTION IN MIXED WET AND LOW IFT SYSTEMS

M. Sohrabi, H. Shahverdi, M. Jamiolahmady, M. Fatemi, S. Ireland and G. Robertson
Institute of Petroleum Engineering, Heriot-Watt University, Edinburgh, Scotland

This paper was prepared for presentation at the International Symposium of the Society of Core Analysts held in Halifax, Nova Scotia, Canada, 4-7 October, 2010

ABSTRACT

There is significant uncertainty associated with the selection of three-phase relative permeability in particular for the numerical simulations of water-alternating-gas (WAG) injection. Generally, three-phase relative permeabilities are calculated from empirical correlations, which are based on two-phase relative permeabilities. WAG injection involves drainage and imbibition processes taking place sequentially. Therefore, accurate prediction of the relative permeability (kr) functions and their hysteresis effects applicable to WAG are extremely complex. The problem of 3-phase kr selection becomes even more difficult for three-phase systems involving mixed-wet rocks and low gas-oil IFT (interfacial tension) fluids (nearly-miscible fluids).

We use the results of coreflood experiments carried out on two different cores (one water-wet and one mixed-wet) using a low IFT gas-oil system to generate two-phase and three-phase relative permeability data by using an in-house three-phase coreflood simulator.

The results show that water and gas three-phase kr values depend on two independent saturations, contrary to the inherent assumption in most of the existing empirical kr models. Three-phase water, oil and gas kr values were all significantly lower than their corresponding two-phase values. This reduction in kr was more profound for the gas where the three-phase krg was an order of magnitude lower than its corresponding two-phase krg. Using the laboratory derived three-phase kr data, the performance of some of the existing three-phase kr models were evaluated by comparing the results of the WAG experiments with predictions made by a commercial reservoir simulator. In general, considerable discrepancies between the measured and the predicted kr values were observed. Some models performed better than others but no single model was capable of matching all experimental results adequately.

The results of this work highlights some of the complexities involved in determining representative three-phase kr and some of the shortcomings and uncertainties associated with some of the current three-phase kr models particularly for very low-IFT gas and WAG injection. The study clearly demonstrate the need for further integrated experimental and modeling investigations of three-phase flow and the need for

developing improved physics-based methodologies and models for better characterization of three-phase flow and particularly for the numerical simulation of WAG injection.

INTRODUCTION

Relative permeability values describe the comparative ease by which different fluids flow in a porous medium. Prediction of the performance of most enhanced oil recovery processes, such as tertiary gas injection and water-alternating-gas (WAG) injection, requires knowledge of three-phase relative permeabilities. Considerable efforts have been directed towards gaining a better understanding of three phase flow in porous media and in particular determination of three-phase relative permeability values. However, an accurate estimation of three-phase relative permeability still remains a challenging task for practicing reservoir engineers.

Compared to high IFT systems, very few reports of low IFT gas/oil/water kr measurements are available in the open literature and hence the knowledge of the impact of lower IFTs on three phase relative permeabilities remains very limited. Near-miscible (low IFT) gas injection can happen in a wide range of gas injection processes in oil reservoirs including high pressure hydrocarbon gas injection, CO_2 injection, and multiple contact miscibility. Sohrabi et al[4] demonstrated that the pore-scale mechanisms of flow of very low IFT gas/oil systems are significantly different from high IFT gas/oil systems. The results of their high-pressure micromodel experiments revealed that very high oil recovery can be achieved by near-miscible gas injection. The results were also confirmed by a series of coreflood experiments of near-miscible gas and WAG injection (Sohrabi et al [5]).

Three-phase relative permeabilities are usually calculated from empirical correlations, which are based on the corresponding two-phase relative permeability data. Furthermore, when these correlations are applied, most simulators implicitly assume that the reservoir is a water-wet system and oil is the intermediate-wetting phase with the gas being non-wetting phase. Therefore the oil relative permeability is a function of two saturations, Kro (Sg, Sw). This further implies that water and gas three phase relative permeabilities depend only on their own saturations, i.e. the three phase quantities, Krw = Krw (Sw) and Krg = Krg (Sg). Many experiments indicate, however, that reservoirs are not strongly water-wet but can attain a wide variety of wettability states in which certain clusters of pores are water-wet and others are oil-wet. For these wettability states the saturation-dependencies for the corresponding three-phase relative permeabilities are not systematically known. The problem of reliable three-phase relative permeability estimation becomes more difficult for three-phase system with a very low gas-oil IFT (near-miscible systems). Odd Steve Hustad[3] proposed a three-phase kr model (the ODD3P model), addressing the state of wettability of the porous medium in which water and gas kr as well as kro are functions of two saturations. Also in the ODD3P method, the relative permeability of each phase is scaled by the corresponding interfacial tension to account for the impact of IFT and miscibility condition.

The objective of the Water-Alternating-Gas (WAG) Injection project at Heriot-Watt University is to obtain an improved understanding of the WAG injection process through an integrated experimental and simulation study and to develop methodologies and models by which three-phase relative permeabilities applicable to WAG particularly for near-miscible gas/oil in mixed-wet rocks can be well defined and estimated. Three-phase displacement experiments using near-miscible fluids and mixed-wet cores are being carried out to experimentally examine the processes of water, gas, WAG and SWAG injection and to generate laboratory measured data for modeling and simulation of these processes. The results of the coreflood experiments are used for examining the suitability of various three-phase relative permeability models and for developing improved models and methodologies. An in-house three-phase coreflood simulator has been developed and is being used to obtain three-phase relative permeabilities directly from three-phase coreflood experiments by history matching the production/injection and pressure differential data obtained in the laboratory.

EXPERIMENTAL AND SIMULATION RESULT

Core Flood Experiments

The objective of the coreflood experiments was two fold. First, to observe the behavior of three-phase systems especially in mixed-wet cores and at near-miscible conditions (low gas/oil IFT values). Second, to generate experimentally measured data that can be used to develop three-phase relative permeability models applicable to mixed-wet near-miscible systems, particularly for WAG processes. Therefore, a series of gas-oil, water-oil, three-phase (gas, oil and water), WAG and SWAG (simultaneous injection of water and gas) injection experiments were carried out. The displacement experiments were initially carried out in a 1-Darcy (high permeability) Clashach core. To examine the impact of capillary forces on the flow and the relative permeability of different phases, a 65 mD (lower permeability) core is now being used as well. The dimensions and properties of both cores are given in Table 1.

The hydrocarbon fluid system used in the coreflood experiments was prepared from a binary mixture of methane (C1) and *n*-butane (*n*-C4). To eliminate mass transfer during the displacement experiments, all the fluids (oil, gas and brine) were pre-equilibrated at the test pressure and temperature of 1840 psia and 100°F and were kept under these conditions in high-pressure transfer vessels and in a temperature-controlled oven. Table shows the measured properties of the fluid system at the conditions of the experiments. The critical point pressure of the hydrocarbon mixture (mixture of C1 and n-C4) was about 1865 psia and hence, at the pressure of the experiments (1840 psi), the system was very close to its critical point and hence nearly miscible[8].

We have developed a three-phase core flood simulator, based on genetic algorithm which was used to determine three-phase kr curves by matching the fluid recovery and differential pressure data obtained from three-phase displacement core tests. The core flood simulator provides best estimates of three-phase relative permeabilities based on suitable mathematical functions defined to describe their dependency to phase saturations. In our approach, no assumptions are made regarding the dependency of the multiphase flow functions to a specific saturation. The simulator generates 2D tables for three-phase relative permeability of each phase. Representative functions of three-phase kr of each phase including oil, water and gas is assumed to be dependent on two saturation functions. This assumption is in contrast with the intrinsic assumption in most of the existing three-phase kr models (e.g. Stones) which assume that only the intermediate wetting phase's kr is a function of two independent saturations (e.g. kro = kro (Sw, Sg)) while the wetting and non-wetting phase kr are functions of their own saturations (i.e. krw = krw (Sw), krg = krg (Sg)). This point is particularly important for simulation of three-phase flow in mixed-wet or weakly-wet systems which are believed to be more realistic wettability conditions of oil reservoirs instead of the assumption of strongly water-wet or oil-wet conditions. It should be noted that the estimated kr values obtained from history matching of the displacement experiments are more accurate and reliable in the vicinity of the saturation trajectory in which the fluid displacements occurred.

High permeability core

A series of more than 20 complete two-phase and three-phase coreflood experiments has been performed so far on a 1000 mD mixed wet core, mainly at unsteady state and some at steady state conditions. The wettability of the core was changed by aging the core in a crude oil which resulted in a stable and lasting mixed-wet condition. Detailed experimental data such as fluid production profiles, the pressure drop across the core and the fluid saturations were used in the core flood simulator to derive two-phase and three-phase relative permeability data. The experiments include water flooding, gas and oil injection, WAG and SWAG injection. Table 3 lists some of these experiments and the initial saturation of fluids at the beginning of each experiment. The experiments were successfully history matched using our coreflood optimizer to obtain kro, krw and krg. The saturation path during each tests is described in Table 3 and presented in Figure 1.
Three-phase kr is presented as a matrix (two dimensional table) where the first row and column of the matrix represent two independent fluid saturations and the middle points of this matrix are the corresponding 3-phase kr values, i.e. $k_{ro} = k_{ro}$ (S_w, S_g), $k_{rw} = k_{rw}$ (S_o, S_g), $k_{rg} = k_{rg}$ (S_w,S_o). However, to plot three-phase kr values in XY graphs one the phase's saturation must be kept constant and plot kr in terms of the saturation of the other phase.

The kro and krg data obtained from a two-phase gas injection experiment in the presence of connate water saturation and those obtained from a three-phase gas injection experiment at the initial oil and water saturations of 60% and 40% respectively (Soi=0.60, Swi=0.40) are shown in Figure 2 and Figure 3 respectively. As can be clearly seen from these Figures, 3-phase relative permeability of oil and gas are very different from their 2-phase relative permeabilities. This comparison demonstrates that there is little relevance between the values of 2-phase and 3-phase kr values with 3-phase relative permeability being substantially lower than their corresponding 2-phase values.

In this case, the 3-phase kro was around 30% of 2-phase kro and the 3-phase krg was only around 10% of the 2-phase krg values. In other words, the dependency of 3-phase krg on two independent saturations is more pronounced than that of 3-phase kro. This observation contradicts the common assumption that in a three-phase system the most non-wetting phase (usually gas) relative permeability is only a function of its own saturation. Comparison between the estimated krw from 2-phase and 3-phase water injection experiments (Swi = 0.40, Soi=0.43) is shown in Figure 4. A significant difference is observed between these two krw curves revealing that the 3-phase krw also depends on two saturation values.

To examine the impact of hysteresis on three-phase relative permeabilities, the three-phase kr curves obtained from the experiments carried out in different saturation directions were compared with each other as shown in Figure 5 to Figure 8. Figure 5 depicts 3-phase kro at a constant water saturation (Sw=40%) obtained from oil and gas injection (fourth and fifth experiments in Table 3). It is noted that at the same saturation of three flowing phases, kro of the oil injection test is higher than kro of the gas injection test. This difference highlights the importance of the kr path dependency i.e. hysteresis experienced in these two tests. The impact of hysteresis on krg obtained from these two tests is illustrated in Figure 6. As can be seen, at the same saturation of three flowing phases, drainage krg (gas injection) is much higher than the imbibition krg (oil injection). By comparing Figure 5 and Figure 6 it can be concluded that the hysteresis of the gas phase is much more pronounced than that for the oil phase. 3-phase krw obtained from oil and water injection tests (sixth and ninth test in Table 3) are plotted in Figure 7. Figure 8 presents 3-phase krw obtained from the gas and water injection tests (the third and eighth test in Table 3) which show no hysteresis effect for krw and the difference between krw obtained from different tests at the same saturation of three flowing phases is minimal.

<u>Low permeability core</u>

A set of two-phase and three-phase (WAG) displacements were conducted on the 65 mD core under water-wet conditions. The main objective of working with this lower permeability core (65 mD compared to 1000 mD) was to examine the impact of capillary forces on the flow and relative permeability of different phases by comparing the results with those obtained for high-permeability core. The oil-gas Pc (capillary pressure) was assumed to be negligible (due to a very low gas/oil IFT) whereas the oil-water Pc was used in the simulation. As the core was long (compared to core plugs usually used for these measurements) and the injection rate was relatively high, capillary end effect was assumed to be negligible. The initial saturation of fluids at the beginning of the low-permeability coreflood experiments that will be discussed in this paper is given in Table 4.

First, a series of two-phase displacement experiments were carried out. The aim of these experiments was to obtain the two-phase kr curves necessary for obtaining three-phase kr from the existing models and also for comparing the performance of these models against the laboratory derived three-phase kr values. One of the displacement types that occur in the reservoir during the WAG process is the displacement of oil by the gas slugs. To determine the gas-oil relative permeability curves applicable to this displacement type, an unsteady-state gas injection test was carried out (first test in Table 4). The gas injection experiment began with the core containing 82% oil and 18% irreducible water saturation (Swi=18%). Then, gas injection commenced initially at a rate of 50 cm^3/h. For simulating WAG process, it is equally important to obtain imbibition gas/oil kr curves as well as the drainage ones. During WAG injection in an oil reservoir, an oil bank can form, which can displace the gas left behind from a previous gas injection cycle and hence the imbibition gas-oil kr curves would be needed for simulating this process. Thus, an oil injection experiment (second test in Table 4) was performed. The oil injection started with an initial injection rate of 50 cm^3/h and later the injection rate was increased to 100 cc/hr (to increase the range of saturation in the experiment). A water injection test (third test in Table 4) was designed to generate data for two-phase water/oil relative permeability curves for our system in the imbibition direction. Another relevant displacement types in the context of WAG injection is the displacement of mobile water by the oil bank, which forms as a result of alternating injection of water and gas. To determine drainage water-oil relative permeability curves applicable to the displacement of water by oil, an oil injection test (fourth test in Table 4) was carried.

All the above two-phase experiments were then successfully simulated by the in-house coreflood simulator to obtain kr values for different imbibition and drainage processes. Figure 9 shows a comparison between the imbibition and drainage relative permeability of the oil-gas system at irreducible water saturation (Swi=18%). As can be seen, there is a considerable difference between the gas-oil kr values obtained by gas injection compared to the gas-oil kr values obtained by oil injection in the same oil/gas/rock system. The difference in the oil and gas kr values obtained in different saturation direction is significant even for the oil phase which is the wetting phase in this system. It is noted that as the gas is the non-wetting phase, its hysteresis is more than that of oil. As would be expected, the oil relative permeability k_{ro} obtained from the oil injection test (increasing oil saturation) is higher than that obtained from the gas injection experiment (decreasing oil saturation k_{rog}) whereas the imbibition gas relative permeability (k_{rgo}) is far less than its drainage counterpart (k_{rgo}). Figure 10 shows the results of a similar comparison but for the oil-water system for both drainage and imbibition processes. These water-oil kr curves also confirm that both the wetting (water) and non-wetting (oil) phase kr exhibit strong dependency on saturation direction, albeit, this difference is more pronounced for non-wetting phase. Comparing the results obtained for the oil-gas system (Figure 9) and the oil-water system (Figure 10), shows that in this low permeability rock, both the gas-oil and the oil-water systems show kr dependency on saturation direction however, the effect is much more pronounced for gas-oil system.

The two-phase kr curves obtained from the experiments have been used to calculate three phase kr values by using some of the existing three-phase kr models available in commercial reservoir simulators (e.g. StoneI[6], StoneII[7], StoneExponent[2] and Saturation Weighted Interpolation[1]). These estimated 3-phase kr values were then used to simulate the results of a near-miscible WAG injection experiment carried out in the 65 mD core using Eclipse reservoir simulator. The oil and brine production obtained from the first cycle of the gas injection (fifth displacement in Table 4) from the experiment and from numerical simulations (Eclipse) using different three-phase models are shown in Figure 11 and Figure 12, respectively. As can be seen, there is a large variation in prediction of different models used. The closest prediction of the produced oil obtained in the experiment for the first gas injection period was obtained by the StoneExponent model (using Exponent=2) whereas for the brine production the STONE2 model has resulted in a better prediction amongst the 3-phase kr models used.

After the 1st period of gas injection which was carried out following an initial water flooding period, the WAG experiment continued with a 2nd water injection period (sixth displacement in Table 4). The results of this 2nd water injection period were again simulated using Eclipse. The oil and gas production obtained from the experiment and the simulation of the 2nd cycle of water injection are presented in Figure 13 and Figure 14 respectively. Using the StoneExponent model very good agreement was achieved with the oil recovery profile obtained in the laboratory but by using Exponent=10 rather than Exponent=2 that was used for matching the oil recovery in the 1st gas injection (Figure 11). The produced gas obtained in the laboratory in this 2nd cycle of water injection was best matched by using Stone1 compared to other models used.

After the 1st cycle of gas and water injection, the 2nd cycle began with another gas injection period. Comparisons of the results obtained for the 2nd gas injection period (last displacement in Table 4) from the experiment and from numerical simulation using different three-phase kr models are presented in Figure 15 and Figure 16. As can be seen, all of the three-phase kr models used in this comparison significantly underestimate the amount of oil recovery obtained during the 2nd gas injection cycle. Since the gas used in this WAG injection experiment has a very low IFT (0.04 mNm^{-1}) with the oil, after the breakthrough of the gas, still significant amount of oil recovery takes place (Sohrabi *et al*, 2007). This physics is not captured by the existing three-phase kr models and hence the significant underestimation of the amount of oil recovery as shown in Figure 15. The STONE EXPONENT model (with exponent 0.01) gave better oil recovery prediction compared to the other models used, nevertheless, the quality of the oil recovery prediction for the 2nd gas injection cycle was poor specially for the latter parts of this gas injection period whereas the produced brine predicted by the saturated weighted interpolation model led to the closest match of the measured brine production.

CONCLUSIONS

A series of two-phase and three-phase displacement experiments, including water injection, gas injection (at different saturation direction) and WAG injection, was carried out in two different cores (a 1000 mD mixed-wet and a 65 mD water-wet core) using a three-phase fluid system with a very low gas/oil IFT (0.04 mNm^{-1}). The results of the experiments were used to evaluate the performance of various injection strategies and in particular WAG injection performance in cores with one order of magnitude difference in permeability. The results were also used to generate two-phase and three-phase kr experimentally. These laboratory-derived kr values were used to first, examine the performance of the existing three-phase kr models by comparing the results of the numerical simulation of the experiments with the measured data. Second, the data and the improved knowledge gained from this integrated experimental and theoretical work are being used to develop improved methodologies for obtaining three-phase kr values.

The following conclusions can be drawn from this work:

High permeability (1000 mD) mixed-wet core

1- Relative permeability of all phases under 3-phase flow conditions are functions of two independent fluid saturations. This contradicts the oversimplifying assumptions made in most of the widely used empirical 3-phase relative permeability models neglecting this dependency.
2- The three-phase kr obtained for different phases show little relevance to the two-phase kr ones. In our experiments, significant reduction (up to an order of magnitude) of phase relative permeability was observed when moving from two-phase to three-phase flow.
3- Three-phase krg exhibit higher hysteresis effect than kro whereas 3-phase krw from different core flood tests do not show significant dependency on the saturation history, hysteresis.
4- Due to the high tendency of gas to become trapped during the injection of the wetting phase, the drainage 3-phase krg is larger than the imbibition 3-phase krg while kro in an oil injection (imbibition) test is higher than that in a gas injection (drainage) test.

Low permeability (65 mD) water-wet core

1- Despite having a very low interfacial tension (IFT=0.04 MNm-1) between the oil and gas, the impact of hysteresis was considerable in the 65 mD core and ignoring kr hysteresis could lead to highly erroneous results in numerical simulation. This is attributed to stronger capillary forces in lower permeability rock.
2- Comparing the performance of different kr models in numerical simulation of the WAG experiment carried out in the 65 mD core revealed that no single model could adequately match all the measured data. However, some performed better that the others. The STONE EXPONENT model could produce a good match of the oil recovery profile of the 1st gas injection and the subsequent (2nd) water injection but it underestimated the brine recovery of the 1st gas injection and the gas recovery of the subsequent (2nd) water injection.
3- None of the models could produce the characteristic continued oil recovery during low-IFT gas injection which is an important feature of low-IFT (near miscible) gas injection.

ACNOWLEDGMENT
This work was carried out as part of the Water-Alternating-Gas (WAG) Injection JIP at Heriot-Watt University. The WAG consortium at Heriot-Watt University is equally sponsored by, Statoil, BHP Billiton, Chevron, Dong Energy, Petrobras and the UK Department of Energy and Climate Change (DECC), which is gratefully acknowledged.

REFERENCES
1- Baker, L.E. “Three-Phase Relative Permeability Correlations”, SPE17369, Tulsa, Oklahama, April 1988.
2- Hustad, O.S. and Holt,T.”Gravity Stable Displacement of Oil by Hydrocarbon Gas after Waterflooding”. SPE/DOE Eighth Symposium on Enhanced Oil Recovery, Tulsa, Oklahoma, April 1992, SPE 24116.
3- Hustad, O.S. “A Coupled Model for Three-Phase Capillary Pressure and Relative Permeability”. SPE Journal, Page 59-69 , March 2002, SPE 74705.
4- Sohrabi M., Danesh A., Tehrani, D. and Jamiolahmady M.,” Microscopic Mechanisms of Oil Recovery by Near-Miscible Gas Injection”, Transport in Porous Media, July 2007a.
5- Sohrabi, M., Tehrani, D. H. and Al-Abri, M., "Performance of Near-Miscible Gas and SWAG Injection in a Mixed-Wet Core”, proceedings of the International Symposium of the Society of Core Analysts, Calgary, Canada, 10-13 September 2007b.
6- Stone, H.L, “Probability Model For Estimating Three-Phase Relative Permeability”, J. Pet. Tech, (Feb 1970) 22, 214-218; Trans., AIME (1970), 249, 214-218.
7- Stone, H.L, “Estimation of Three-Phase Relative Permeability and Residual Oil data”, J.Can.Pet.Tech, v.12, No. 4 (Oct-Dec. 1973), 53-61.
8- WAG 3 Final Reports, Institute of Petroleum Engineering, Heriot-Watt University.

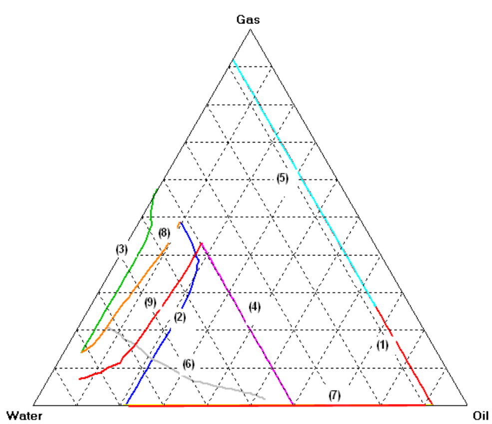

Figure 1: Experimental Saturation path obtained from experiments (1000mD) described in Table 3

Table 4: coreflood tests into 65 mD water-wet core

No	Soi	Sgi	Swi	Experiment
1	0.82	0.00	0.18	Gas Injection (2Phase)
2	0.00	0.82	0.18	Oil Injection (2Phase)
3	0.82	0.00	0.18	Water Injection (2Phase)
4	0.00	0.00	1.00	Oil Injection (2Phase)
WAG Injection				
5	0.82	0.00	0.18	1st Water Injection
6	0.42	0.00	0.58	1st Gas Injection
7	0.30	0.23	0.47	2 nd Water Injection
8	0.26	0.16	0.58	2 nd Gas Injection

Table 1: Core properties

-------------------Mixed wet core------------------	
Length (cm)	61.3
Diameter (cm)	4.86
Pore volume (cc)	200
Porosity(%)	17.7%
Absolute Permeability(mD)	1000
Swi(%)	8%
-------------------Water wet core------------------	
Length (cm)	60.5
Diameter (cm)	5.082
Pore volume (cc)	223
Porosity(%)	18.8%
Absolute Permeability(mD)	65
Swi(%)	18%

Table 2: Fluid properties at 1840psia and 37.8C

Properties	Oil	Gas	Water
Density (g/cc)	0.317	0.211	0.98
Viscosity (cp)	0.0405	0.0249	0.68
Interfacial tension (mN/m)	Oil/gas = 0.04		

Table 3: coreflood tests into 1000 mD mixed wet core

No	Soi	Sgi	Swi	Experiment
1	0.92	0.000	0.08	Gas Injection (2phase)
2	0.210	0.000	0.790	Gas Injection (3phase)
3	0.041	0.140	0.819	Gas Injection (3phase)
4	0.600	0.000	0.400	Gas Injection (3phase)
5	0.000	0.574	0.426	Oil Injection (3phase)
6	0.069	0.207	0.724	Oil Injection (3phase)
7	0.920	0.000	0.080	Water injection (2phase)
8	0.095	0.488	0.417	Water injection (3phase)
9	0.170	0.430	0.400	Water injection (3phase)

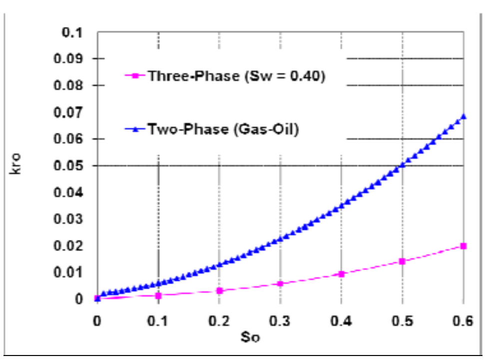

Figure 2: Effect of water saturation kro obtained from the 2-phase gas injection 3-phase gas injection (Soi=0.60, Swi=0.40), test 1 and 4 in Table 3

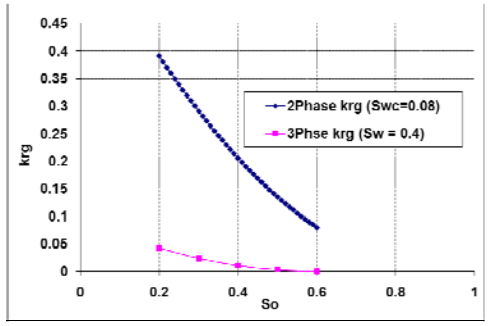

Figure 3: 2-phase and 3-phase krg obtained from the 2-phase and 3-phase (Soi=0.60, Swi=0.4) gas injection.),test 1 and 4 in Table 3.

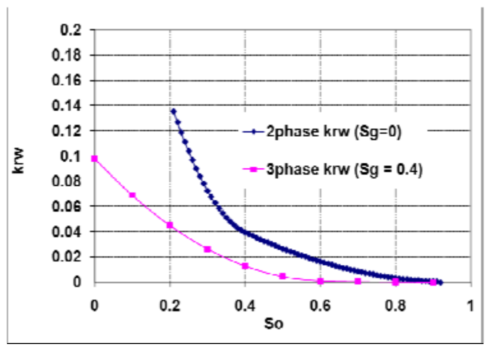

Figure 4: 2-phase and 3-phase krw obtained from 2-phase and 3-phase (Swi = 0.40, Sgi=0.43) water injection.,tests 7 and 9 in Table 3.

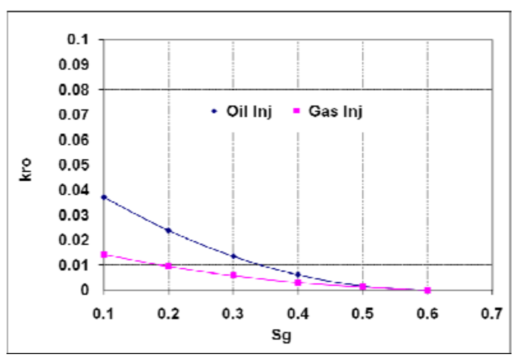

Figure 5: 3-phase kro obtained from oil injection (at Sgi =57.4%, Swi = 42.6%) and gas injection tests (at Swi= 40%, Soi=60%) , both at constant Sw=40%.

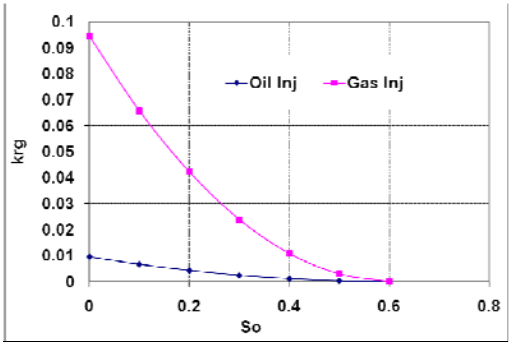

Figure 6: 3-phase krg obtained from oil injection (at Sgi =57.4%, Swi = 42.6%) and gas injection (at Swi= 40%, Soi=60%), both at constant Sw=40%. (tests 4 and 5 in Table 3)

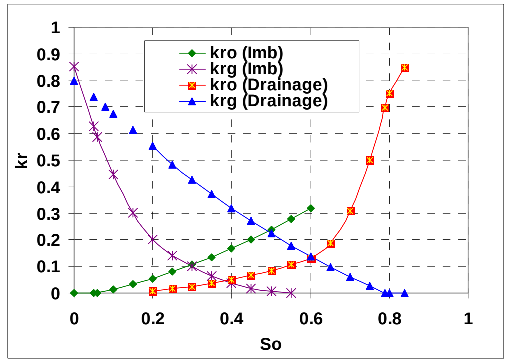

Figure 9: Comparison between imbibition and drainage kr (with Swi) for oil-gas system and water-wet core (65mD) obtained from first and second experiment given in Table 5.

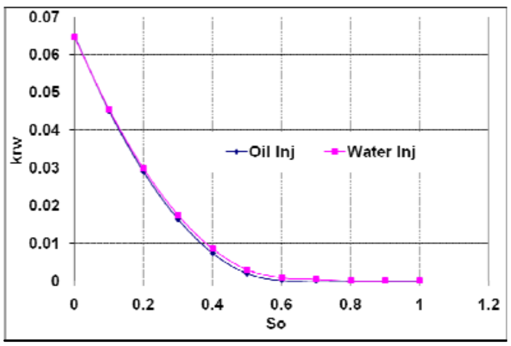

Figure 7: 3-phase krw obtained from oil injection (at Sgi =21%, Swi = 72.5%) and water injection (at Sgi= 43%, Soi=17) both at constant Sg=20%.(tests 6 and 9 in Table 3)

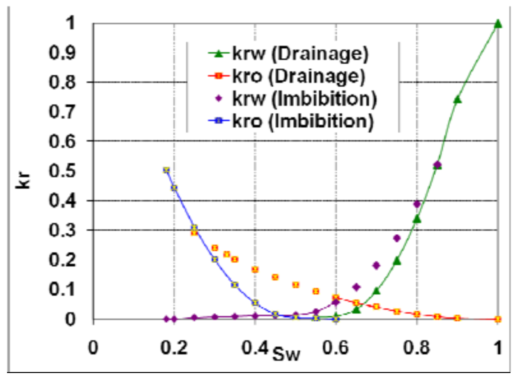

Figure 10: Comparison between imbibition and drainage kr for oil-water system and water-wet core (65 mD) obtained from third and fourth experiment given in Table 6.

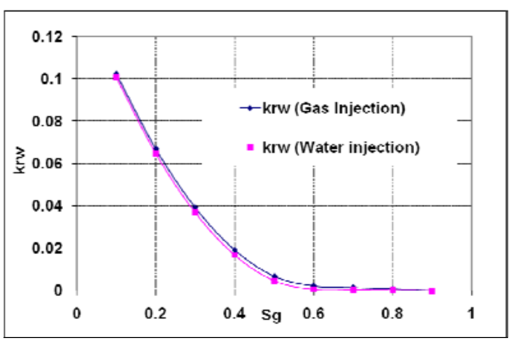

Figure 8: 3-phase krw obtained from gas injection (at Swi =82%, Soi = 4%) and water injection (at Sgi= 48.8%, Soi=9.5%) injection tests , both at constant So=10%.(tests 3 and 8 in Table 3)

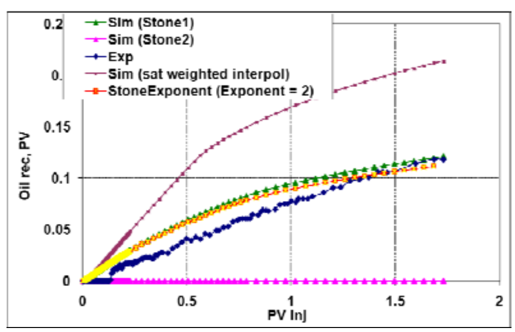

Figure 11: Comparison experimental oil recovery obtained from the first cycle of gas injection with those resulted from simulation using different three-phase kr model available in Eclipse100.

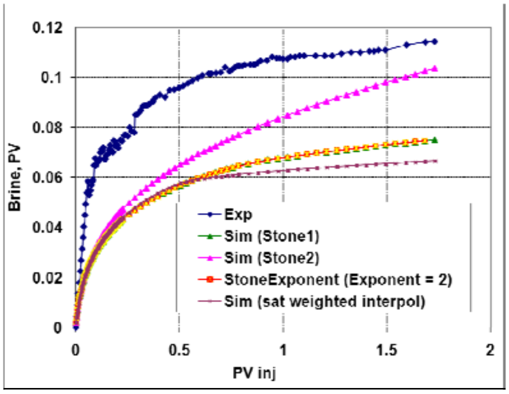

Figure 12: Comparison experimental brine recovery obtained from the first cycle of gas injection with those resulted from simulation using different three-phase kr models available in Eclipse100.

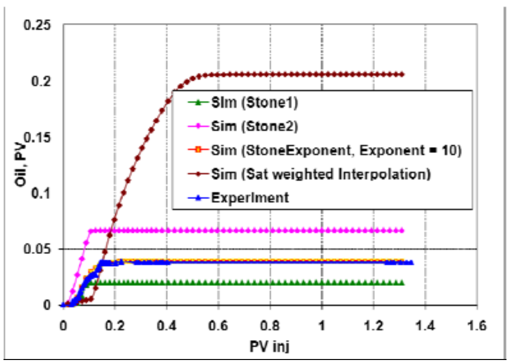

Figure 13: Comparison experimental oil recovery obtained from the second cycle of water injection with those resulted from simulation using different three-phase kr model available in Eclipse100.

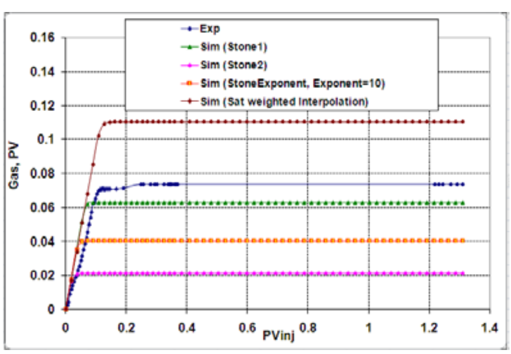

Figure 14: Comparison experimental gas recovery obtained from the second cycle of water injection with those resulted from simulation using different three-phase kr model available in Eclipse100.

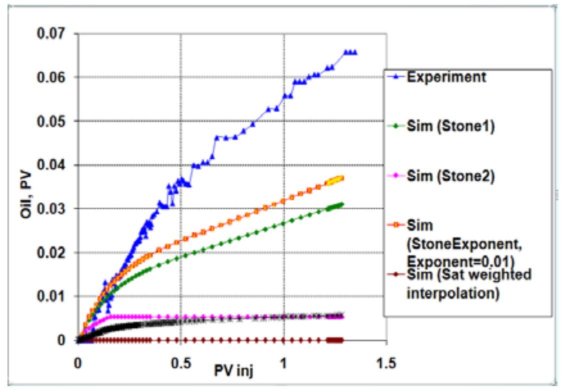

Figure 15: Comparison experimental oil recovery obtained from the second cycle of gas injection with those resulted from simulation using different three-phase kr model available in Eclipse100.

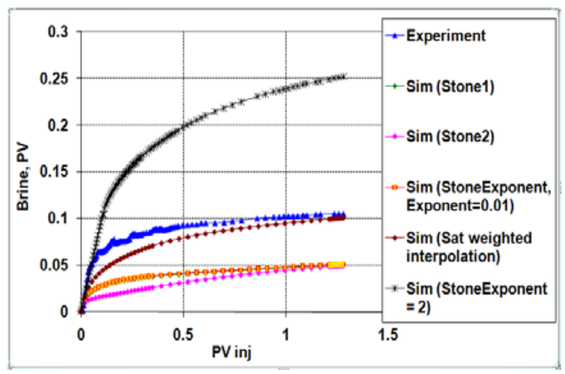

Figure 16: Comparison experimental brine recovery obtained from the second cycle of gas injection with those resulted from simulation using different three-phase kr model available in Eclipse100.